



## Origami multiple paper-based electrochemical biosensors for pesticide detection



F. Arduini<sup>a,\*</sup>, S. Cinti<sup>a</sup>, V. Caratelli<sup>a</sup>, L. Amendola<sup>b</sup>, G. Palleschi<sup>a</sup>, D. Moscone<sup>a</sup>

<sup>a</sup> Department of Chemical Science and Technologies, University of Rome Tor Vergata, Via della Ricerca Scientifica, 00133 Rome, Italy

<sup>b</sup> ArpaLazio, Via Giuseppe Saredo 52, 00173 Rome, Italy

### ARTICLE INFO

#### Keywords:

Butyrylcholinesterase  
Alkaline phosphatase  
Tyrosinase  
Paraoxon  
2,4-dichlorophenoxyacetic acid  
Atrazine

### ABSTRACT

Herein, we propose the first three-dimensional origami paper-based device for the detection of several classes of pesticides by combining different enzyme-inhibition biosensors. This device was developed by integrating two different office paper-based screen-printed electrodes and multiple filter paper-based pads to load enzymes and enzymatic substrates. The versatile analysis of different pesticides was carried by folding and unfolding the filter paper-based structure, without any addition of reagents and any sample treatment (i.e. dilution, filtration, pH adjustment). The paper-based platform was employed to detect paraoxon, 2,4-dichlorophenoxyacetic acid, and atrazine by exploiting the capability of these different types of pesticides (i.e. organophosphorus insecticides, phenoxy-acid herbicides, and triazine herbicide) to inhibit butyrylcholinesterase, alkaline phosphatase, and tyrosinase, respectively. The degree of inhibition correlating to the quantity of pesticides was evaluated by chronoamperometrically monitoring the enzymatic activity in the absence and in the presence of pesticides by using a portable potentiostat. To improve the sensitivity, the paper-based electrodes were modified with carbon black alone in the case of platforms for 2,4-dichlorophenoxyacetic acid and atrazine detection, or decorated with Prussian blue nanoparticles for the detection of paraoxon. The paper-based device was applied for the detection of paraoxon, 2,4-dichlorophenoxyacetic acid, and atrazine at ppb level in both standard solutions and river water sample. The accuracy of this origami multiple paper-based electrochemical biosensor was evaluated in river water by recovery studies, obtaining satisfactory values (e.g. for paraoxon  $90 \pm 1\%$  and  $88 \pm 2\%$ , for 10 and 20 ppb, respectively). The proposed three-dimensional origami paper device allows for rapid, cost-effective and accurate pesticide detection in surface water as a result of combining filter and office papers, screen-printing, wax-printing and nanomaterial technology.

### 1. Introduction

Pesticides are largely used at worldwide level to improve the food production, fulfilling the needs of the global population, which is increasing year by year. Although persistent pesticides (e.g. dichlorodiphenyltrichloroethane (DDT)) have been replaced with less persistent ones, contamination of food, soil and water by pesticides remains an issue of public concern. To better manage this problem, EU sets regulations for a sustainable employment of pesticides by promoting the adoption of Integrated Pest Management (Directive 2009/128/EC). However, the sales of pesticides in EU during 2011–14 have increased, reaching 395,628 t of active ingredients, demonstrating that the widespread use of pesticides is still an ongoing problem (Eurostat, 2016). The criticism on pesticides is also highlighted in the frame of European Water Policy, pesticides such as chlorfenvinphos, chlorpyrifos, atrazine have been established in the

priority list of hazardous substances (Directive 2008/105/EC). In this overall scenario, the detection of pesticides in water at low concentrations (ppb level) is required to accomplish the regulatory aspect and to preserve the health of environment and human beings. The detection of pesticides is usually carried out by using liquid chromatography or gas chromatography coupled to mass-spectrometric detection; however, these methods require laboratory set-up, expensive instrumentations, skilled personnel, and often the use of organic solvents, producing unsafe waste. To avoid the aforementioned drawbacks, in the last few years several electrochemical biosensors have been developed (Ren et al., 2017a, 2017b), offering such advantages as cost effectiveness, ease in use, miniaturised devices and suitability for in situ applications, in agreement with 11th principle of Green Chemistry (Anastas and Warner, 1998). For toxic compound detection, electrochemical biosensors based on enzyme inhibition have attracted tremendous attention in the scientific community because they are able to

\* Corresponding author.

E-mail address: [fabiana.arduini@uniroma2.it](mailto:fabiana.arduini@uniroma2.it) (F. Arduini).

<https://doi.org/10.1016/j.bios.2018.10.014>

Received 2 July 2018; Received in revised form 23 September 2018; Accepted 9 October 2018

Available online 13 October 2018

0956-5663/ © 2018 Elsevier B.V. All rights reserved.

provide information about the presence of environmental pollutants as well as food contaminants in a timely fashion and off-laboratory setting.

This type of biosensors is based on the monitoring of the enzymatic activity in absence and in presence of an inhibitor, generating a reduced response in the presence of pollutants owing to an inhibited enzymatic activity by pesticides.

There have been efforts dedicated to develop printed electrochemical biosensors for the detection of pesticides in surface water by exploiting several enzymes, depending on the pesticides of interest (Arduini et al., 2006; Haddaoui and Raouafi, 2015; Bollella et al., 2016).

Recent applications of technologies to the design of electrochemical (bio)sensors for environmental analysis have promoted the development of novel, easier and more environmentally friendly devices (Arduini et al., 2017). In this regard, paper-based electrochemical (bio)sensors have paved the way for sustainable measurements of analytes, using paper as an active substrate where reagents are stored, electrodes are printed, real-life samples are analysed without any sample treatment and avoiding the use of organic solvents (Cinti et al., 2016; Weng et al., 2018; Wang et al., 2018). Furthermore, paper is a cost-effective and easy-to-handle support for developing microfluidic devices without requiring any instrumentation as miniaturised pump for microfluidic management (Kumar et al., 2015). Despite the recent employment of paper in the construction of electrochemical biosensors (Dungchai et al., 2009; Nie et al., 2010; Lamas-Ardisana et al., 2018; Sun et al., 2018), few examples reported in literature are customised for pesticide detection (Meredith et al., 2016; Ding et al., 2016). In this regard, we have reported an integrated paper-based screen-printed electrochemical biosensor for quantifying organophosphates, using paraoxon as a model compound (Cinti et al., 2017) without any sample treatment i.e. filtration, dilution, reagents addition. Motivated by the outstanding features of the paper and by the need to seek an analytical tool able to detect multiclassses of pesticides for smart environmental monitoring, we here report the first integrated multiple paper-based electrochemical biosensors in a 3D-origami configuration for pesticide detection based on enzyme inhibition, exploiting the versatility of origami approach (Liu and Crooks, 2011; Liu et al., 2012; Li et al., 2014). This paper-based platform is constituted of two different electrodes printed on office paper connected to several filter paper pads to deliver multiple analyses in term of i) initial and residual enzymatic activity, ii) detection of different pesticides using different enzymes immobilised on a paper-based lab-on-chip.

## 2. Experimental section

### 2.1. Reagents and equipment

Alkaline phosphatase from bovine intestinal mucosa, butyrylcholinesterase from horse serum, tyrosinase from mushroom, atrazine, diethylamine, n,n-dimethylformamide, 2,4 dichlorophenoxyacetic acid (2,4-D), ferric chloride, hydrochloric acid, magnesium chloride, paraoxon, triethanolamine, sodium chloride, potassium ferricyanide, potassium dihydrogen phosphate, dipotassium hydrogen phosphate were purchased from Sigma Aldrich. MO, USA. S-butyrylthiocholine chloride was purchased by Santa Cruz Biotechnology, Inc. TX, USA, while catechol from Aldrich Chem. Carbon black (CB) N220 was kindly supplied as a gift from Cabot Corporation, Ravenna, Italy which is characterised by carbon nanoparticles as showed in Fig. S1. Cyclic voltammetry and chronoamperometry were carried out using a portable PalmSens Instrument (PalmSens, Netherlands) in connection with a laptop. Micrographs of paper-based materials and paper-based electrodes were acquired by means of a field emission gun scanning electron microscopy (FEG-SEM, Leo Supra 35). The TEM image was recorded with a Philips CM120 Analytical instrument (LaB6).

### 2.2. Production of carbon black dispersion

The dispersion of carbon black (CB) was prepared by adding 20 mg of CB powder to 20 mL of solvent (a mixture of dimethylformamide (DMF): water (1:1)), and sonicated for 60 min at 59 kHz (Arduini et al., 2012).

### 2.3. Production of carbon black/Prussian blue nanocomposite powder

A carbon black/Prussian blue nanoparticles (CB/PBNPs) nanocomposite was previously characterised and prepared following our previous paper (Cinti et al., 2014). Briefly, 1 g of carbon black powder was suspended in a 10-mL solution containing 0.1 M potassium ferricyanide prepared in 0.01 M HCl. After 5 min of stirring, 10 mL of 0.1 M ferric chloride, prepared in 0.01 M HCl, was added, and the resulting suspension was stirred for 10 min. CB decorated with PB nanoparticles (CB/PBNPs) were collected by centrifugation, and washed five times with 0.01 M HCl. The precipitate was then dried in an oven at 100 °C for 1.5 h. The carbon black/Prussian blue nanoparticles were then used to prepare a dispersion using the same procedure described in Section 2.2.

### 2.4. Fabrication of the paper-based biosensor

A semi-circular pattern initially designed using the drawing software Adobe Illustrator was printed on a piece of Fabriano Copy 2 office paper (80 g/m<sup>2</sup>) by using an office wax printer (ColorQube) to create a hydrophobic pattern. The wax-printed paper was then placed in a 100 °C oven for 4 min to allow the wax to diffuse through the paper, producing a hydrophobic region, which defines the hydrophilic zone. A three-electrode system (screen-printed electrode, SPE) was manually screen-printed using an Ag/AgCl ink (Electrodag 477 SS) to print the pseudo-reference electrode, and a graphite-based ink (Electrodag 421) to print the working and counter electrodes on hydrophilic zone. All the conductive-inks were purchased from Acheson (Italy) (Colozza et al., 2018). Successively, the electrodes printed on office paper were modified with a carbon black or a carbon black/Prussian blue nanoparticle dispersion by drop casting. In the case of SPEs used for the detection of atrazine and 2,4 dichlorophenoxyacetic acid (2,4-D), 2 µL of the carbon black dispersion was applied to the working electrode surface. After that, the solvent was allowed to volatilize at room temperature, leaving a CB “film” onto the electrode surface. In the case of SPEs used for the detection of paraoxon, the SPEs were modified with the carbon black/Prussian blue nanoparticle dispersion as described for carbon black dispersion. The same wax-printing procedure was used for preparing a hydrophobic pattern on a piece of filter paper (67 g/m<sup>2</sup>, Cordenons, Italy). The porosity of this type of paper, depicted in Fig. S2, has been exploited to load the enzyme as well as the substrate, while the morphology of office paper (Fig. S2) to print the electrodes. Successively, the strips constituted of four pads loaded with different enzymes and substrates, depending of the pesticides to detect, were integrated with the electrode printed on office paper using an adhesive tape. The morphology of the working electrode printed on office paper modified with nanomaterials (e.g carbon black) is similar with the one (Arduini et al., 2015) observed in case of polyester-based printed sensor modified with carbon black (Fig. S2). After the preparation, the origami paper-based device has been used within the day. It is possible to use the paper-based system within one week, maintaining the pad under vacuum and including the use of nitrogen flow before closing the reservoir that contains the device, being butyrylthiocholine highly hygroscopic and easily hydrolysed. Regarding the working stability, the same office paper-based sensor both modified with carbon black or carbon black/Prussian blue nanoparticles can perform at least four successive measurements (Figs. S3 and S4).

For paraoxon detection, the red pad (Fig. 1) was loaded with 2 µL of BChE 1 U/mL solubilised in phosphate buffer 0.05 M + KCl 0.1 M,

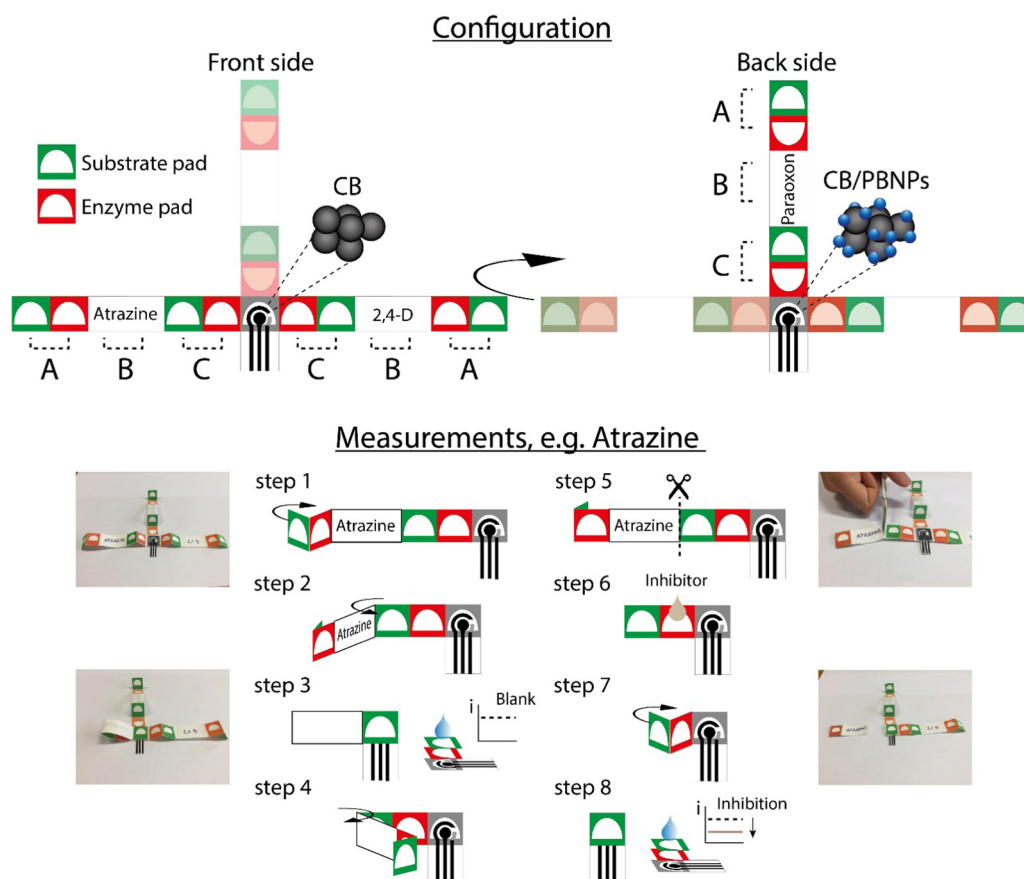


Fig. 1. Schematic representation and photographs of the configuration of the paper-based platform and measurement procedure.

pH = 7.4, while the green pad was loaded with 20  $\mu\text{L}$  of butyrylthiocholine 10 mM solubilised in phosphate buffer 0.05 M + KCl 0.1 M, pH = 7.4.

For 2,4-D quantification, the red pad (Fig. 1) was loaded with 2  $\mu\text{L}$  of alkaline phosphatase 50 U/mL solubilised in TRIS buffer 0.03 M +  $\text{MgCl}_2$  5 mM + NaCl 0.05 mM, pH = 7.6, while the green pad was loaded with 20  $\mu\text{L}$  of 1-naphthyl phosphate 10 mM solubilised in DEA buffer 0.97 M +  $\text{MgCl}_2$  0.01 M + KCl 0.15 M, pH = 9.8.

For atrazine measurement, the red pad (Fig. 1) was loaded with 2  $\mu\text{L}$  of tyrosinase 25 U/mL solubilised in phosphate buffer 0.05 M + KCl 0.1 M, pH = 6.5, while the green pad was loaded with 20  $\mu\text{L}$  of catechol 0.3 mM solubilised in phosphate buffer 0.05 M + KCl 0.1 M, pH = 6.5.

For the detection of pesticides in real-life sample, the pesticides were added to river water aliquots and the degree of inhibition was calculated by adding directly the spiked river water sample to the pad.

### 2.5. Measurements of pesticides using the paper-based platform

For the initial enzymatic activity, a pair of green and red pads was put in contact and 20  $\mu\text{L}$  of the distilled water was added; thereafter the enzymatic reaction occurs, and the electroactive enzymatic by-product was detected at the selected applied potential by chronoamperometry. For the residual enzymatic activity, 5  $\mu\text{L}$  of the inhibitor solution (a standard solution or a real-life sample) were loaded onto the red pad (second couple); after 5 min, the green pad was put in contact with the red pad and the printed electrode, and the measurement was carried out as described for the initial enzymatic activity measurement. The chronoamperometric signal was recorded after 100 s. The inhibition percentage was evaluated by using the following equation (Amine et al., 2016):

$$I\% = [(I_0 - I_i)/I_0] \times 100 \quad (1)$$

where  $I_0$  and  $I_i$  represent the biosensor response in terms of enzymatic activity in the absence and in the presence of pesticides.

## 3. Results and discussion

### 3.1. Device concept, configuration and measurement

The origami multiple paper-based biosensor was developed by exploiting the capability of different types of pesticides including paraoxon, 2,4-dichlorophenoxyacetic acid, and atrazine to inhibit the corresponding enzyme of butyrylcholinesterase, alkaline phosphatase, and tyrosinase (Arduini et al., 2010a; Mazzei et al., 2004; Tortolini et al., 2016). To measure the amount of pesticides present in water samples, the concentration of pesticides was quantified using Eq. (1). Fig. 1 illustrates the configuration of the platform, which consists of two office paper-based electrodes printed on the front and the backside of the origami system. The two sensors correspond to a carbon black/Prussian blue nanoparticle dispersion modified graphite working electrode for the detection of thiocholine, which is the enzymatic by-product of butyrylcholinesterase, and a carbon black modified graphite working electrode for the detection of 1-naphthol and 1,2-benzoquinone, which are the enzymatic by-products of either alkaline phosphatase or tyrosinase. To deliver a reagent-free analytical tool, different strips of filter paper containing several pads were linked with the electrodes printed on office paper by adhesive tape. Each strip is constituted of two pairs of different pads (A, C in Fig. 1), two pads containing the enzyme (red pads), the other two pads containing the substrate (green pads), separated by an empty piece of paper (B in Fig. 1).

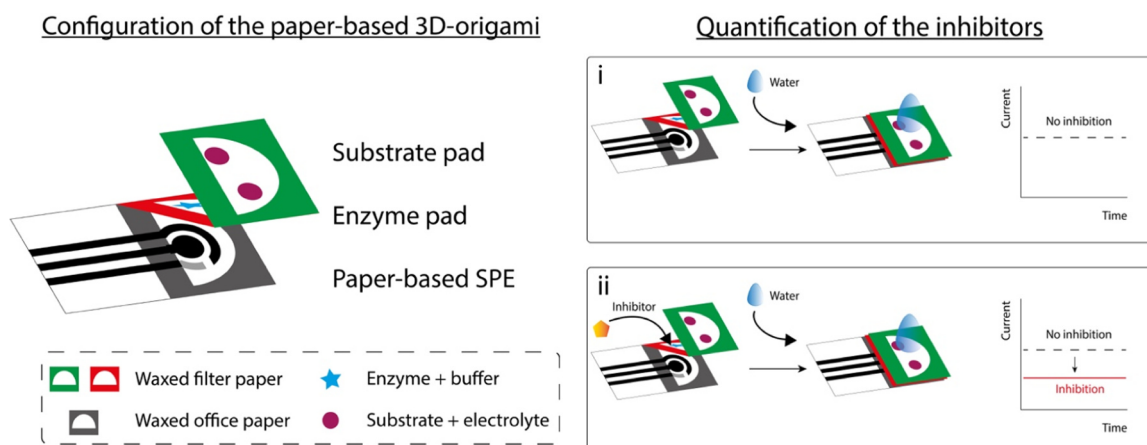


Fig. 2. Details of the enzymatic activity measurement using electrodes printed on office paper combined with a multi-pad system.

For measuring the initial enzymatic activity ( $I_0$ ) e.g. atrazine measurement, the distal couple of pads is used, and the green pad containing the substrate is folded firstly to come in contact with the red pad containing the enzyme (step 1), then further folded (step 2) in order to be both put into intimate contact with the electrochemical cell printed on office paper (step 3). After that, 20  $\mu\text{L}$  of distilled water were added to the origami sensor and the measurement started, since the distilled water wets the pads containing enzyme, substrate, buffer salts, dissolving them and producing a solution with the selected optimal working conditions for enzymatic reaction (i.e. pH, ionic strength). The enzymatic reaction took place on with the formation of the enzymatic by-product (1,2-benzoquinone), which was reduced at working electrode surface to yield the current  $I_0$ .

To perform the measurement of a sample, the already used pads were open and cut (step 4–5) and 5  $\mu\text{L}$  of water sample were loaded only onto the red pad containing the enzyme of the C pair (step 6). After an incubation time of 5 min, the green pad was folded to sandwich the red one so that both were in an intimate contact (step 7–8) with the electrochemical cell printed on office paper for measuring the residual enzymatic activity ( $I_i$ ), quantified as reported before (Fig. 2). Repeating this procedure with the three strips of pads present in the platform, six measurements can be carried out with the same paper-based device, delivering an integrated analytical tool able to quantify three different types of pesticides.

### 3.2. Paraoxon detection using BChE paper-based biosensor

For the detection of organophosphorus insecticides such as paraoxon, we selected BChE as biocomponent as it is irreversibly inhibited by organophosphates. This enzyme is able to hydrolyse the natural substrate butyrylcholine, with the production of electro-inactive butyric acid and choline as enzymatic by-products. To develop a sensitive amperometric biosensor and avoid the use of a more expensive bi-enzymatic biosensor, as well as the low sensitivity of a potentiometric detection, butyrylthiocholine was used as a synthetic substrate, to produce thiocholine that is electroactive and can be amperometrically detected. Because the oxidation of thiol compound is characterised by fouling problem at the working electrode surface, we exploited Prussian blue (ferric hexacyanoferrate) nanoparticles combined with carbon black because of its capability to electrocatalyse the oxidization of thiocholine at low applied potential, overcoming the fouling problem which occurs at bare carbon electrodes (White et al., 2002). To evaluate the suitability of the electrode printed on office paper modified with carbon black/Prussian blue, a cyclic voltammetric study was carried out using bare and modified electrodes with butyrylthiocholine and BChE (Fig. 3A). In the case of the bare SPE, in presence of enzymatic product thiocholine, only a small increase of the oxidative current was observed

at the potential close to 0.6 V. In the presence of the substrate butyrylthiocholine, carbon black/Prussian blue nanoparticle modified SPE yielded a pair of redox peaks observed at around 0.2 V and 0.3 V, which were assigned to the reduction of Prussian blue to Prussian white and the oxidation of Prussian white back to Prussian blue, respectively (Fig. 3A). In the presence of thiocholine, which is generated by the reaction between butyrylcholinesterase and butyrylthiocholine, an increase in the anodic peak current was observed, compared to response without butyrylthiocholine. The increase in the anodic peak current observed, compared to response without butyrylthiocholine, is ascribed to the rise in concentration of Prussian white at the electrode surface, resulting in an increase of the anodic peak current. By contrast, the cathodic peak is proportional to Prussian blue concentration, which diminishes at the electrode surface by the reaction with thiocholine. In this way, the obtained cyclic voltammeteries highlighted the typical behaviour of oxidative reaction catalysed by the electrochemical mediator, demonstrating the suitability of this sensor to detect the thiocholine enzymatic by-product.

#### 3.2.1. Optimisation of the experimental parameters

Once the effectiveness of carbon black/Prussian blue nanoparticle-SPEs was verified, several parameters including BChE concentration, the amount of butyrylthiocholine to load on pad, and the reaction time were optimised to obtain a sensitive, repeatable, and time-saving platform. All the chronoamperometric studies for the BChE biosensors were performed at 0.3 V (vs. Ag/AgCl) as applied potential, taking into account the cyclic voltammetric study and our previous results (Cinti et al., 2017).

**3.2.1.1. Optimisation of the volume of Butyrylthiocholine to load on the pad.** Since the paper-based platform is conceived as the integration of electrode printed on office paper and filter paper multipads, it was necessary to evaluate the loading capacity of the pad e.g. amount of substrate to load on the pad. Several volumes (i.e. 10, 20 and 30  $\mu\text{L}$ ) of 10 mM of butyrylthiocholine were cast on the pad. A volume of 20  $\mu\text{L}$  was selected since it gave the higher response and the best repeatability, as depicted by Fig. S5.

**3.2.1.2. Optimisation of BChE concentration.** Successively, BChE concentration was optimised by testing three different concentrations, namely 2 mU, 20 mU, 200 mU (Fig. 3B). Since the inhibition of butyrylcholinesterase by paraoxon is of irreversible type, the degree of inhibition depends on the enzyme concentration (Arduini and Amine, 2014). To seek high sensitivity, the enzyme concentration should be chosen as the lowest amount of enzyme able to furnish a measurable signal, thus 20 mU was selected for the rest of the work.

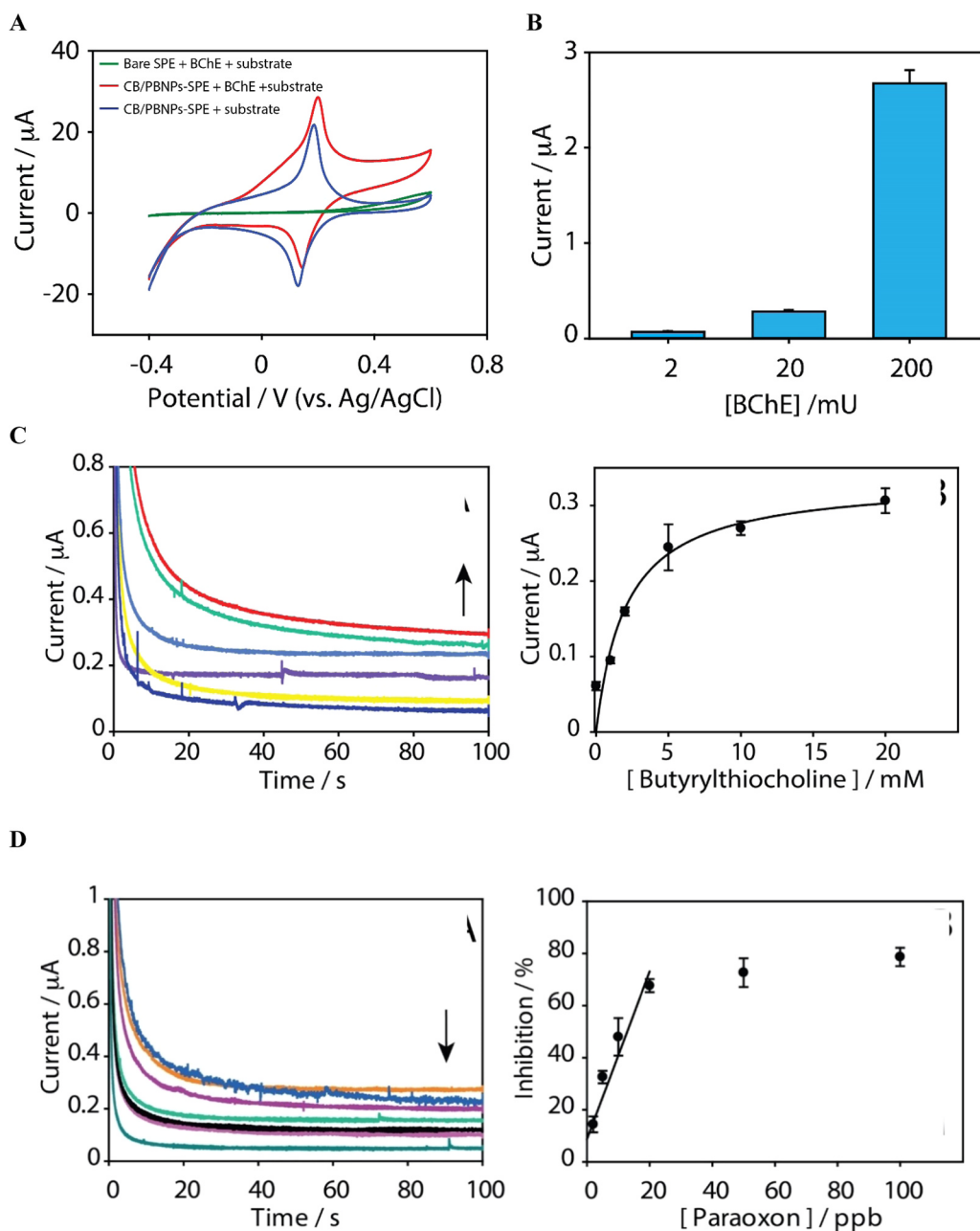


**Fig. 3.** BChE paper-based biosensor for paraoxon detection. **A)** Cyclic voltammeteries using bare SPE (green line) and CB/PBNPs-SPE (red line) in presence of BChE 200 mU and butyrylthiocholine 10 mM, while the cyclic voltammeter of CB/PBNPs-SPE in presence only of butyrylthiocholine 10 mM is reported in blue line, scan rate 50 mV/s. **B)** Optimisation of enzymatic unit to load on the filter-paper pad. Chronoamperometric measurement at an applied potential of 0.3 V vs Ag/AgCl pseudoreference using 10 mM of butyrylthiocholine and reaction time of 2 min. **C)** Chronoamperometric measurement at an applied potential of 0.3 V vs Ag/AgCl pseudoreference, reaction time of 2 min, using 20 mU of BChE cast on red pad varying butyrylthiocholine concentration on green pad and the corresponding calibration curve. **D)** Chronoamperometric measurement at an applied potential of 0.3 V vs Ag/AgCl pseudoreference, reaction time of 2 min, using 20 mU of BChE cast on red pad and butyrylthiocholine 10 mM cast on the green pad varying the concentration of paraoxon, on the right of Fig. 3D the calibration curve. Measurements recorded in triplicate. The black arrows in Fig. 3C and D indicate the trend of the response at the increasing of analyte concentration. (For interpretation of the references to color in this figure legend, the reader is referred to the web version of this article)

**3.2.1.3. Optimisation of the reaction time.** The next optimised parameter was the reaction time, which is the time of reaction between the enzyme and the substrate needed to obtain the enzymatic by-product. The effect of three different reaction times was investigated, namely 1, 2, 4 min. As shown in Fig. S6, the reaction time selected was 2 min, as the best compromise in terms of sensitivity and time of analysis.

### 3.2.2. Paper-based platform for substrate detection

Once optimised, the paper-based platform was then tested towards butyrylthiocholine, the enzymatic substrate that was analysed in the range comprised between 1 and 20 mM, observing a Michaelis Menten behaviour (Arduini and Amine, 2014), with a  $K_{Mapp} = (2.3 \pm 0.5)$  mM (Fig. 3C), which is in agreement with the literature data (i.e.  $K_{Mapp} = (2.2 \pm 0.3)$  mM) using BChE immobilised by cross-linking method at a polyester-based sensor (Arduini et al., 2015). The minimum butyrylthiocholine concentration that gives  $V_{max}$  was 10 mM, and it was

chosen for the insecticide determination; in addition, the repeatability of the biosensor was tested at this butyrylthiocholine level with a RSD% equal to 3%, demonstrating a remarkable repeatability.

### 3.2.3. Paper-based platform for paraoxon detection

In order to detect paraoxon, we have exploited the capability of paraoxon to irreversibly inhibit BChE, and thus the decrease of the response due to presence of inhibitor needs to be related with the response in absence of inhibitor using Eq. (1). For this reason, the first measurement using the first couple of red and green pads was carried out for the evaluation of  $I_0$ , i.e. the enzymatic activity quantification in the absence of an inhibitor. After that, the first couple of the pads was cut and the second couple was used to evaluate the response of the inhibited paper-based platform. In details, for the  $I_0$  measurement, the enzymatic activity was evaluated by wetting the sandwiched multipad with 20  $\mu$ L of distilled water, followed by the chronamperometric measurement at applied potential. For the inhibitor

detection, the red pad was firstly wetted with 5  $\mu\text{L}$  of paraoxon, and after 5 min of incubation between BChE and paraoxon (incubation time), the same procedure reported for the  $I_0$  quantification was used to record  $I_i$ . Under the optimal conditions, the paper-based platform was tested with several concentrations of paraoxon in the range between 2 and 100 ppb, observing a linear range up to 20 ppb described by the following equation, inhibition percentage =  $8.7 \pm 2.9 + 3.2 \pm 0.3 \times (\text{paraoxon concentration/ppb})$ , with  $R^2 = 0.907$  (Fig. 3D;  $N = 3$ ), yielding a sensitivity of  $3.2 \pm 0.3$  degree of inhibition/ppb. The limit of detection (LOD) of the biosensor was found equal to 2 ppb, calculated as the 15% of inhibition, which is slightly higher in respect to other works reported in literature based on plastic-based SPE (0.145 ppb) or carbon paste electrode (0.86 ppb) (Joshi et al., 2005; Di Tuoro et al., 2011). To verify the suitability of the paper-based platform with real-life water sample, the water of Aniene River (Aniene, Italy) was collected and analysed without any treatment process, but only by adding 5  $\mu\text{L}$  to the red pad. No inhibition was observed in the real-life matrices, demonstrating the absence of BChE inhibitors at the detection limit level of the device. The calibration plot obtained in matrix showed a linearity up to 20 ppb described by the following equation  $y = (10.5 \pm 1.2) + (1.7 \pm 0.1) x$ , with a  $R^2 = 0.960$  and a sensitivity of  $1.7 \pm 0.1$  degree of inhibition/ppb. Subsequently, the sample was spiked with two levels of paraoxon, namely 10 and 20 ppb, obtaining satisfactory recovery values of  $90 \pm 1\%$  and  $88 \pm 2\%$ , respectively. These results demonstrated the capability of this biosensor to detect paraoxon also in a complex matrix such as untreated river water by an easy procedure and a cost-effective device.

### 3.3. Paper-based platform for 2,4-D detection

The detection of 2,4-D belonging to phenoxy herbicides was carried out measuring the degree of inhibition of alkaline phosphatase because this enzyme is reversibly inhibited by 2,4-D (Mazzei et al., 2004; Bollella et al., 2016). Phosphatases enzymes are capable to catalyze the hydrolysis of phosphoric acid esters, and this group of enzymes is divided in four classes, depending on the chemical nature of the substrate or the type of hydrolysis reaction. The alkaline phosphatase hydrolyses the phosphate ester functional group of its substrates to the respective alcoholic product and among the several substrates that can be employed, 1-naphthyl phosphate was used, giving the electroactive compound 1-naphthol. The detection of this latter is usually carried out by using bulk or miniaturised electrodes such as glassy carbon electrodes and carbon-based screen-printed electrodes, however its measurement is usually associated with electrode fouling processes. In this regard, Wang group demonstrated that the amperometric response of ALP biosensor with 1-naphthyl phosphate as substrate decayed rapidly to zero current, which was explained by the formation of a polymeric layer that caused fouling of the working electrode surface (Preechaworapun et al., 2008). To overcome this problem, in this work we used carbon black nanomaterial as electrode nanomodifier to improve the sensitivity (Deroco et al., 2017, 2018; Wong et al., 2018) as well as to reduce the fouling problem, since in our previous works we demonstrated its anti-fouling properties in the case of thiols, NADH, and also phenolic compounds (Arduini et al., 2010b; Talarico et al., 2015). Fig. 4A shows the cyclic voltammograms at a bare electrode and carbon black-SPE in the presence of 200 mU ALP and 40 mM of 1-naphthyl phosphate, demonstrating the reduction of the applied potential and the increase the sensitivity using carbon black as nanomodifier of the working electrode surface. Furthermore, we demonstrated for the first time that carbon black is able to improve the electroanalytical performance of the SPE also in the case of naphthol measurements, besides the already tested compounds such as NADH,  $\text{H}_2\text{O}_2$ , thiocholine, catechol, caffeic acid (Arduini et al., 2010c, 2012; Talarico et al., 2015), widening the applications of SPE modified with this cost-effective nanomaterial.

#### 3.3.1. Optimisation of the experimental parameters

In the case of reversible inhibition, such as the case of ALP inhibited by 2,4-D, the concentration of enzyme did not affect the degree of

inhibition (if the enzyme concentration is lower than the concentration of the inhibitor), thus the enzyme concentration capable to give a response characterised by high sensitivity and repeatability should be selected (Arduini and Amine, 2014). Chronoamperometric measurements were carried out using different concentrations of ALP, namely 10, 20, 50, 100, 200 mU (Fig. 4B). As expected, the increase of enzyme units cast on the pad leads to an increase of the observed response. Since 100 mU and 200 mU highlight a little variation, 100 mU were selected for the rest of the work, avoiding the misuse of the enzyme. Regarding other parameters such as the reaction time and the volume of the substrate to load, the values were chosen taking into account the optimisation carried out before in the case of paraoxon detection, thus 2 min and 20  $\mu\text{L}$ , respectively. After, the paper-based platform was tested towards the enzymatic substrate, analysed in the range between 5 and 40 mM, observing a Michaelis Menten behaviour with a  $K_{Mapp} = (9.6 \pm 2.0)$  mM (Fig. 4C).

For the substrate concentration, we have selected the amount able to deliver a more repeatable measurement. For this reason, 10 mM of 1-naphthyl phosphate was selected having a RSD% equal to 7%, lower than the RSD% of the other concentrations.

#### 3.3.2. Paper-based platform for 2,4-D detection

Once optimised the selected parameters, the paper-based platform was tested with several concentrations of 2,4-D detection in the range comprised between 100 and 1000 ppb, observing a linear range up to 600 ppb described by the following equation, inhibition percentage =  $22.6 \pm 0.7 + 0.043 \pm 0.002 \times (2,4\text{-D concentration/ppb})$ , ( $N = 3$ ),  $R^2 = 0.970$  (Fig. 4D). The limit of detection of the biosensor was found equal to 50 ppb, calculated as the 25% of inhibition (Amine et al., 2016). To verify the suitability of the paper-based platform with real-life water sample, the water of Aniene River was analysed as above reported, by only adding 5  $\mu\text{L}$  of the real-life water sample to the red pad. No inhibition was observed in this matrix, demonstrating the absence of ALP inhibitors at the detection limit level of the device. The calibration curve obtained in matrix showed a linearity up to 200 ppb with an equation equal to  $y = (14.6 \pm 0.5) + (0.100 \pm 0.004) x$ ,  $R^2 = 0.989$  and a sensitivity of  $0.100 \pm 0.004$  degree of inhibition/ppb. Subsequently, the sample was spiked with two levels of 2,4-D namely 100 and 200 ppb, obtaining satisfactory recoveries of  $86 \pm 4\%$  and  $93 \pm 2\%$ , respectively.

### 3.4. Paper-based platform for atrazine detection

The detection of atrazine was carried out analysing the inhibition degree of tyrosinase enzyme, since this enzyme is inhibited in a reversible way by atrazine (Tortolini et al., 2016). Tyrosinase is a monophenol monooxygenase which catalyses the o-hydroxylation of monophenols to form o-diphenols followed by an oxidative reaction from o-diphenols to o-quinones (Vicentini et al., 2013). The detection of enzymatic activity relies on monitoring the quinone enzymatic by-products, electrochemically reduced to o-diphenols. For the tyrosinase enzymatic activity measurement, the electrode modified with carbon black was employed, taking into account that i) in this way it is possible to use only two paper-based electrodes for the measurements of the three types of pesticides ii) in previous works the suitability of carbon black in the fabrication of tyrosinase-based biosensor has been demonstrated (Arduini et al., 2010c; Ibáñez-Redín et al., 2018).

#### 3.4.1. Optimisation of the experimental parameters

In the case of tyrosinase biosensor development, the applied potential for the reduction of the enzymatic by-product quinone was optimised by investigating three different applied potentials namely  $-100$  mV,  $-150$  mV, and  $-200$  mV. As displayed in Fig. 5A, the potential of  $-150$  mV represents the best compromise between a satisfactory sensitivity and good repeatability (RSD% equal to 2.5%), thus this value was selected in agreement with the results obtained using carbon-black based paste

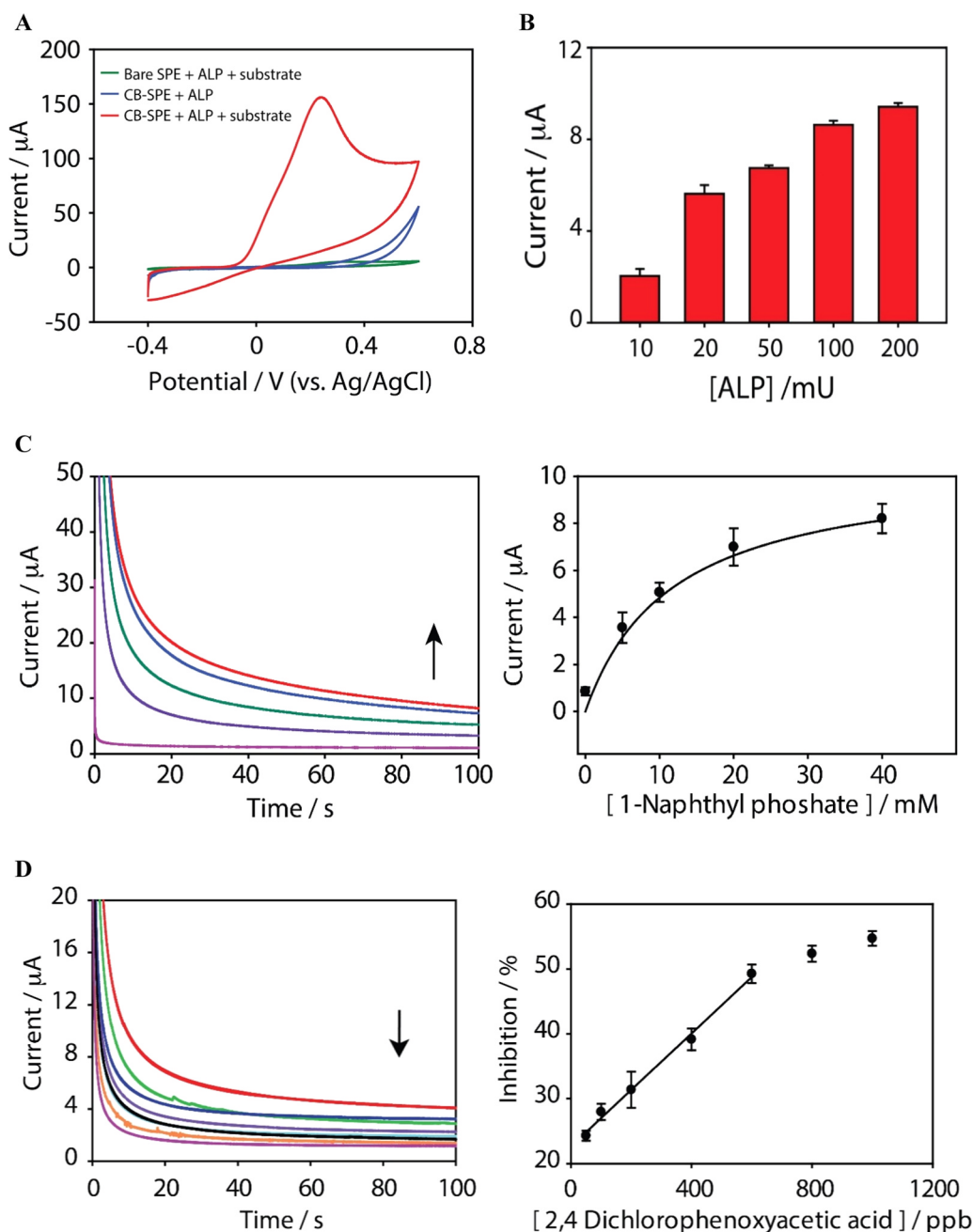


**Fig. 4.** ALP paper-based biosensor for 2,4-D detection. **A)** Cyclic voltammograms using bare SPE (green line) and CB-SPE (red line) in presence of 200 mU ALP and 40 mM of 1-naphthyl phosphate while the cyclic voltammogram of CB-SPE in presence only of 40 mM of 1-naphthyl phosphate is reported in blue line, scan rate 50 mV/s. **B)** Optimisation of enzymatic unit to load on the filter-paper pad. Chronoamperometric measurement at an applied potential of 0.3 V vs Ag/AgCl pseudoreference using 40 mM of 1-naphthyl phosphate and reaction time of 2 min. **C)** Chronoamperometric measurement at an applied potential of 0.3 V vs Ag/AgCl pseudoreference, reaction time of 2 min, using 100 mU of ALP cast on red pad varying 1-naphthyl phosphate concentration on green pad and the corresponding calibration curve. **D)** Chronoamperometric measurement at an applied potential of 0.3 V vs Ag/AgCl pseudoreference, reaction time of 2 min, using 100 mU of ALP cast on red pad and 1-naphthyl phosphate 10 mM cast on the green pad varying the concentration of 2,4-D, on the right of Fig. 4D the calibration curve. Measurements recorded in triplicate. The black arrows in Fig. 4C and D indicate the trend of the response at the increasing of analyte concentration. (For interpretation of the references to color in this figure legend, the reader is referred to the web version of this article)

electrode or using carbon nanotube based-carbon paste electrode (Arduini et al., 2010c; Mita et al., 2007). As in the case of ALP biosensor, the enzymatic units to load on the pad were chosen taking into account that tyrosinase is reversibly inhibited by atrazine. More specifically, five different concentrations of enzyme were evaluated in a range between 10 and 200 mU. As shown in Fig. 5B the best compromise between sensitivity and repeatability was 50 mU, thus this value was selected for the further experiments. The response of biosensor toward the enzymatic substrate was then evaluated in the range of 20  $\mu$ M–1 mM (Fig. 5C), obtaining a  $K_{Mapp}$  equal to  $172 \pm 15 \mu$ M. The value found is the half than the one reported in literature (e.g.  $300 \pm 2 \mu$ M) (Espín et al., 2000), demonstrating the suitability of this biosensor to detect also catechol. In the case of competitive reversible inhibition in nature, the sensitivity of biosensor is improved by using concentration of the enzymatic substrate lower than inhibitor

concentration, thus a lower concentration in respect to the concentration to give the maximum enzymatic rate (i.e. 300  $\mu$ M) characterised by a good repeatability RSD = 4% ( $n = 3$ ) was chosen.

#### 3.4.2. Paper-based platform for atrazine detection

The optimised paper-based platform was then applied to atrazine detection. A linear range between 10 and 100 ppb described by the following equation, inhibition percentage =  $24.5 \pm 1.3 + 0.25 \pm 0.02 \times (\text{atrazine concentration/ppb})$ , with  $R^2 = 0.917$  in real-life river water sampled from Aniene River, as shown in Fig. 5D. Also, as no inhibition was observed in a real-life matrix, the accuracy was evaluated by recovery studies at two levels (i.e. 50 and 100 ppb), achieving recovery values equal to  $80 \pm 4\%$  and  $92 \pm 3\%$ , respectively.

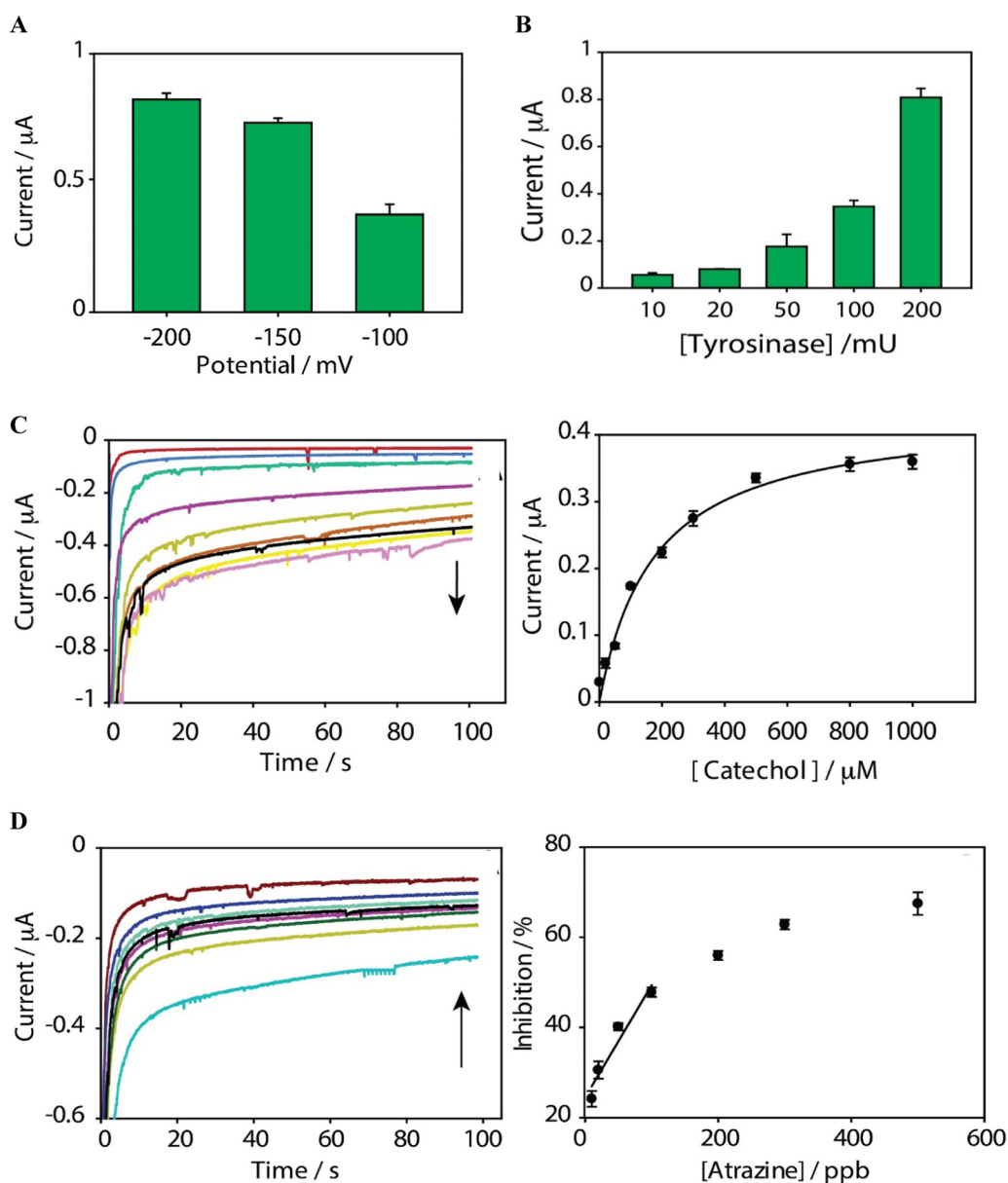


**Fig. 5.** Tyr paper-based biosensor for atrazine detection. **A)** Optimisation of applied potential. Chronoamperometric measurement using 200 mU Tyr cast on the red pad and catechol 10 mM on green pad, reaction time of 2 min **B)** Optimisation of enzymatic unit to load on the filter-paper pad. Chronoamperometric measurement at an applied potential of  $-0.15$  V vs Ag/AgCl pseudoreference using 0.2 mM of catechol and reaction time of 2 min **C)** Chronoamperometric measurement at an applied potential of  $-0.15$  V vs Ag/AgCl pseudoreference, reaction time of 2 min, using 50 mU of Tyr cast on red pad varying catechol concentration on green pad and the corresponding calibration. **D)** Chronoamperometric measurement at an applied potential of  $-0.15$  V vs Ag/AgCl pseudoreference, reaction time of 2 min, using 50 mU of Tyr cast on red pad and catechol 0.3 mM cast on the green pad varying the concentration of atrazine, and on the right of Figure D the calibration curve in real-life river water sampled from Aniene River. Measurements recorded in triplicate. The black arrows in Figure C and D indicate the trend of the response at the increasing of analyte concentration.

#### 4. Conclusions

Herein, we demonstrate for the first time the possibility to detect several classes of pesticides by coupling electrode printed on office papers with multi-pad system. This tool was fabricated by merging different technologies including screen-printing, wax-printing and nanomaterial technology, boosting the eco-design aspect and sustainability of the analytical device, since the sensor can be safely disposed of after measurements, negating electrical/electronic waste. The porosity of filter paper was used to load the enzyme as well as the enzymatic substrate to deliver a reagent free analytical tool, thus an unskilled operator would only need to add a few  $\mu$ L of untreated sample or distilled water to carry out the measurement. In addition, the porosity of the paper was also used to treat the sample, owing to the filtering property of the paper that avoids the contact of river particulates with the working electrode surface. Furthermore, the origami design allowed the development of a single device capable of making several measurements for both initial and residual enzymatic activity estimation in case of three different pesticides, demonstrating the polyedric aspect of 3D paper-based devices. In this way, this device can be considered a valid screening system able to detect toxic compounds inhibiting the enzymes used in this paper-based tool, working as a “family doctor”. Further efforts

will be devoted to exploit filter paper also for pre-concentrating the sample, increasing the sensitivity and reducing the detection limit as well as for a sustainable device which matches also the stricter European legal limit for the surface water.

#### Acknowledgement

This work was supported by NanoSWS project ERANETMED2-72-328 - RQ3-2016 and PRIN 2015FFY97L\_003, Authors acknowledge Prof. Ilaria Cacciotti (University of Rome “Niccolò Cusano”) for SEM characterisation, Prof. E. Bemporad and Dr. Daniele De Felicis for TEM microstructural characterization carried out at the Interdepartmental Laboratory of Electron Microscopy (LIME), University Roma Tre, Rome, Italy.

#### Appendix A. Supporting information

Supplementary data associated with this article can be found in the online version at [doi:10.1016/j.bios.2018.10.014](https://doi.org/10.1016/j.bios.2018.10.014).

## References

- Amine, A., Arduini, F., Moscone, D., Palleschi, G., 2016. *Biosens. Bioelectron.* 76, 180–194.
- Anastas, P.T., Warner, J.C., 1998. *Green Chemistry: Theory and Practice*. Oxford University Press, New York, pp. 30.
- Arduini, F., Ricci, F., Tuta, C.S., Moscone, D., Amine, A., Palleschi, G., 2006. *Anal. Chim. Acta* 580, 155–162.
- Arduini, F., Cinti, S., Scognamiglio, V., Moscone, D., Palleschi, G., 2017. *Anal. Chim. Acta* 959, 15–42.
- Arduini, F., Di Nardo, F., Amine, A., Micheli, L., Palleschi, G., Moscone, D., 2012. *Electroanalysis* 24, 743–751.
- Arduini, F., Amine, A., 2014. *Adv. Biochem. Eng. Biotechnol.* 140, 299–326.
- Arduini, F., Forchielli, M., Amine, A., Neagu, D., Cacciotti, I., Nanni, F., Moscone, D., Palleschi, G., 2015. *Microchim. Acta* 182, 643–651.
- Arduini, F., Amine, A., Majorani, C., Di Giorgio, F., De Felicis, D., Cataldo, F., Amine, A., Moscone, D., Palleschi, G., 2010a. *Electrochem. Comm.* 12, 346–350.
- Arduini, F., Amine, A.F., Moscone, D., Palleschi, G., 2010b. *Microchim. Acta* 170, 193–214.
- Arduini, F., Giorgio, F.D., Amine, A., Cataldo, F., Moscone, D., Palleschi, G., 2010c. *Anal. Lett.* 43, 1688–1702.
- Bollella, P., Fusco, G., Tortolini, C., Sanzò, G., Antiochia, R., Favero, G., Mazzei, F., 2016. *Anal. Bioanal. Chem.* 408, 3203–3211.
- Cinti, S., Talarico, D., Palleschi, G., Moscone, D., Arduini, F., 2016. *Anal. Chim. Acta* 919, 78–84.
- Cinti, S., Minotti, C., Moscone, D., Palleschi, G., Arduini, F., 2017. *Biosens. Bioelectron.* 93, 46–51.
- Cinti, S., Arduini, F., Vellucci, G., Cacciotti, I., Nanni, F., Moscone, D., 2014. *Electrochem. Comm.* 47, 63–66.
- Colozza, N., Kehe, K., Popp, T., Steinritz, D., Moscone, D., Arduini, F., 2018. *Environ. Sci. Pollut. Res.* 1–12.
- Deroco, P.B., Lourencao, B.C., Fatibello-Filho, O., 2017. *Microchem. J.* 133, 188–194.
- Deroco, P.B., Rocha-Filho, R.C., Fatibello-Filho, O., 2018. *Talanta* 179, 115–123.
- Ding, J., Li, B., Chen, L., Qin, W., 2016. A three-dimensional Origami paper-based device for potentiometric biosensing. *Angew. Chem. Int. Ed.* 55, 13033–13037.
- Directive on Environmental Quality Standards, 2009. (Directive 2008/105/EC) Directive/128/E.
- Di Tuoro, D., Portaccio, M., Lepore, M., Arduini, F., Moscone, D., Bencivenga, U., Mita, D.G., 2011. *New Biotechnol.* 29, 132–138.
- Dungchai, W., Chailapakul, O., Henry, C.S., 2009. *Anal. Chem.* 81, 5821–5826.
- Espín, J.C., Varón, R., Fenoll, L.G., Gilabert, M.A., García-Ruiz, P.A., Tudela, J., García-Cánovas, F., 2000. *Eur. J. Biochem.* 267, 1270–1279.
- Eurostat, 2016. Agri-environmental indicator - consumption of pesticides, <[http://ec.europa.eu/eurostat/statistics-explained/index.php/Agri-environmental\\_indicator\\_-\\_consumption\\_of\\_pesticides](http://ec.europa.eu/eurostat/statistics-explained/index.php/Agri-environmental_indicator_-_consumption_of_pesticides)> accessed on July 1st, 2018.
- Haddaoui, M., Raouafi, N., 2015. *Sens. Actuat. B* 219, 171–178.
- Ibáñez-Redín, G., Silva, T.A., Vicentini, F.C., Fatibello-Filho, O., 2018. *Enz. Microb. Technol.* 116, 41–47.
- Li, L., Xu, J., Zheng, X., Ma, C., Song, X., Ge, S., Yua, J., Yan, M., 2014. *Biosens. Bioelectron.* 61, 76–82.
- Liu, H., Crooks, R.M., 2011. *JACS* 133, 17564–17566.
- Liu, H., Xiang, Y., Lu, Y., Crooks, R.M., 2012. *Angew. Chem.* 124, 7031–7034.
- Mita, D.G., Attanasio, A., Arduini, F., Diano, N., Grano, D.G., Bencivenga, U., Rossi, S., Amine, A., Moscone, D., 2007. *Biosens. Bioelectron.* 23, 60–65.
- Joshi, K.A., Tang, J., Haddon, R., Wang, J., Chen, W., Mulchandani, A., 2005. *Electroanalysis* 17, 54–58.
- Kumar, A.A., Hennek, J.W., Smith, B.S., Kumar, S., Beattie, P., Jain, S., Rolland, J.P., Stossel, T.P., Chunda-Liyoka, C., Whitesides, G.M., 2015. *Angew. Chem. Int. Ed.* 54, 5836–5853.
- Lamas-Ardisana, P.J., Martínez-Paredes, G., Añorga, L., Grande, H.J., 2018. *Biosens. Bioelectron.* 109, 8–12.
- Mazzei, F., Botrè, F., Montilla, S., Pilloton, R., Podestà, E., Botrè, C., 2004. *J. Electroanal. Chem.* 574, 95–100.
- Meredith, N.A., Quinn, C., Cate, D.M., Reilly, T.H., Volckens, J., Henry, C.S., 2016. *Analyst* 141, 1874–1887.
- Nie, Z., Nijhuis, C.A., Gong, J., Chen, X., Kumachev, A., Martinez, A.W., Narovlyanskaya, M., Whitesides, G.M., 2010. *Lab Chip* 10, 477–483.
- Preechaworapun, A., Dai, Z., Xiang, Y., Chailapakul, O., Wang, J., 2008. *Talanta* 76, 424–431.
- Ren, X., Ma, H., Zhang, T., Zhang, Y., Yan, T., Du, B., Wei, Q., 2017a. *ACS Appl. Mater. Inter.* 9, 37637–37644.
- Ren, X., Zhang, T., Wu, D., Yan, T., Pang, X., Du, B., Lou, W., Wei, Q., 2017b. *Biosens. Bioelectron.* 94, 694–700.
- Sun, X., Wang, H., Jian, Y., Lan, F., Zhang, L., Liu, H., Ge, S., Yu, J., 2018. *Biosens. Bioelectron.* 105, 218–225.
- Talarico, D., Arduini, F., Constantino, A., Del Carlo, M., Compagnone, D., Moscone, D., Palleschi, G., 2015. *Electrochem. Commun.* 60, 78–82.
- Tortolini, C., Bollella, P., Antiochia, R., Favero, G., Mazzei, F., 2016. *Sens. Actuat. B* 224, 552–558.
- Vicentini, F.C., Janegitz, B.C., Brett, C.M., Fatibello-Filho, O., 2013. *Sens. Actuat. B* 188, 1101–1108.
- Wang, H., Jian, Y., Kong, Q., Liu, H., Lan, F., Liang, L., Ge, S., Yu, J., 2018. *Sens. Actuat. B* 257, 561–569.
- Weng, X., Ahmed, S.R., Neethirajan, S., 2018. *Sens. Actuat. B* 265, 242–248.
- White, P.C., Lawrence, N.S., Davis, J., Compton, R.G., 2002. *Electroanalysis* 14, 89–98.
- Wong, A., Santos, A.M., Silva, T.A., Fatibello-Filho, O., 2018. *Talanta* 183, 329–338.